

# A novel mouse model of *in situ* stenting

Janet Chamberlain<sup>1\*</sup>, Mark Wheatcroft<sup>1</sup>, Nadine Arnold<sup>1</sup>, Henry Lupton<sup>2</sup>,  
David C. Crossman<sup>1</sup>, Julian Gunn<sup>1†</sup>, and Sheila Francis<sup>1†</sup>

<sup>1</sup>Department of Cardiovascular Science, School of Medicine and Biomedical Sciences, Floor L, Medical School, Beech Hill Road, Sheffield S10 2RX, UK; and <sup>2</sup>Brivant Medical Engineering, Galway, Ireland

Received 30 January 2009; revised 3 July 2009; accepted 21 July 2009; online publish-ahead-of-print 25 July 2009

Time for primary review: 14 days

<b>Aims</b>	Animal models of stenting are mostly limited to larger animals or involve substantial abdominal surgery in rodents. We aimed to develop a simple, direct model of murine stenting.
<b>Methods and results</b>	We designed a miniature, self-expanding, nitinol wire coil stent that was pre-loaded into a metal stent sheath. This was advanced into the abdominal aorta of the mouse, via femoral access, and the stent deployed. In-stent restenosis was investigated at 1, 3, 7, and 28 days post-stenting. The model was validated by investigation of neointima formation in mice deficient in signalling via the interleukin-1 receptor (IL-1R1), compared with other injury models. Ninety-two per cent of mice undergoing the procedure were successfully stented. All stented vessels were patent. Inflammatory cells were seen in the adventitia and around the stent strut up to 3 days post-stenting. At 3 days, an early neointima was present, building to a mature neointima at 28 days. In mice lacking IL-1R1, the neointima was 64% smaller than that in wild-type controls at the 28-day timepoint, in agreement with other models.
<b>Conclusion</b>	This is the first description of a successful model of murine <i>in situ</i> stenting, using a stent specifically tailored for use in small thin-walled arteries. The procedure can be undertaken by a single operator without the need for an advanced level of microsurgical skill and is reliable and reproducible. The utility of this model is demonstrated by a reduction in in-stent restenosis in IL-1R1-deficient mice.
<b>Keywords</b>	Mouse stent model

## 1. Introduction

*In vivo* models of stenting have been limited to large and medium-sized animals, such as pigs and rabbits, with the porcine model of stenting accepted as the 'gold standard' pre-clinical model.<sup>1,2</sup> A limitation of the latter is that 'normal' pigs do not suffer from atherosclerosis, even when fed a high-fat diet. In comparison, mice are amenable to genetic manipulation, and ApoE-deficient and LDL receptor-deficient mice are susceptible to atherosclerosis.<sup>3,4</sup> In addition, the wide availability of mouse-specific reagents easily facilitates basic science research. Until very recently, however, mice have not been amenable to stent studies due to size

constraints. An arterial stent graft model in the mouse has been described,<sup>5</sup> although this is limited by the advanced level of microsurgical skill required. In addition, this model is not directly comparable with the routine stent insertion methods used in the clinic. Thus, we aimed to develop a simple, direct model of murine stenting deploying stents *in situ*. We designed a miniature self-expanding coil stent for use in the mouse abdominal aorta and evaluated the vascular response to injury.

Interleukin-1 (IL-1) is an apical mediator in signalling cascades and has previously been shown to be important in response to vascular injury in mice<sup>6</sup> and pigs.<sup>7</sup> In the latter study, an inhibitor of IL-1 administered using osmotic pumps reduced in-stent restenosis

\* Corresponding author. Tel: +44 114 2713696, Fax: +44 114 2268898, Email: j.chamberlain@sheffield.ac.uk

† These two individuals are joint senior authors.

Published on behalf of the European Society of Cardiology. All rights reserved. © The Author 2009. For permissions please email: journals.permissions@oxfordjournals.org.

The online version of this article has been published under an open access model. Users are entitled to use, reproduce, disseminate, or display the open access version of this article for non-commercial purposes provided that the original authorship is properly and fully attributed; the Journal, Learned Society and Oxford University Press are attributed as the original place of publication with correct citation details given; if an article is subsequently reproduced or disseminated not in its entirety but only in part or as a derivative work this must be clearly indicated. For commercial re-use, please contact journals.permissions@oxfordjournals.org.

after 28 and 90 days. We confirm in this study the importance of IL-1 in vascular response to stenting, and validate our new model, by observing a reduction in in-stent restenosis after deploying stents in IL-1 receptor (IL-1R1)-deficient mice.

## 2. Methods

### 2.1 Animals

IL-1R1<sup>-/-</sup> mice (stock no. 003245) and their genetically matched wild-type strain, IL-1R1<sup>+/+</sup> (stock no. 000664), were obtained from the Jackson Laboratories. Animals were housed in a controlled environment with a 12 h light/dark cycle at 22°C. All experiments were performed in accordance with the UK legislation under the 1986 Animals (Scientific Procedures) Act, and approval was granted by the University Ethics Review Board. The investigation conforms with the Guide for the Care and Use of Laboratory Animals published

by the US National Institutes of Health (NIH Publication No. 85-23, revised 1996).

### 2.2 Stent design

A self-expanding coil stent made from nitinol wire (Figure 1A) contained within a hollow tubular steel introducer catheter (custom made by Brivant Medical Engineering, Galway, Ireland) was used throughout this study. To deploy, the introducer is retracted over a pusher allowing the stent to deploy to a coil length of 3 mm and diameter of 1 mm (Figure 2A). As the stent exits the catheter eccentrically, the tip was blunted with a laser welded bead and a straight 'leg' added to act as a stabilizing strut lying against the vessel wall during deployment, giving the stent a total length of 4 mm.

### 2.3 Mouse aortic stent procedure

The stent is placed into the abdominal aorta via femoral access (Figure 2B). Mice (27–35 g; 4–6 months old) were pre-treated for

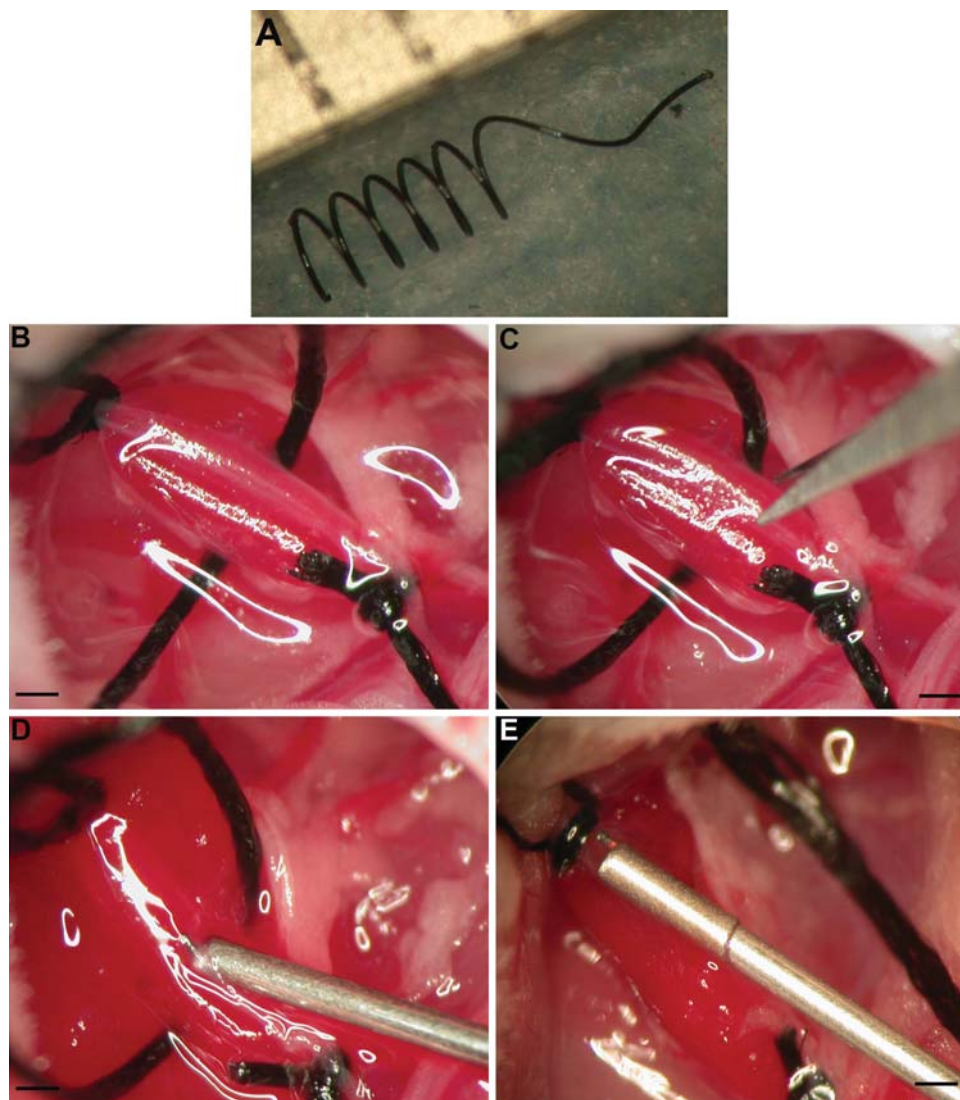


**Figure 1** The stent design. Scale shows 1 mm (A). The femoral vein and artery are controlled proximally by slings and ligated distally (B). Making an arteriotomy (C). The stent catheter is inserted into the femoral artery (D) and slowly advanced (E) into the abdominal aorta. Scale bar represents 350  $\mu$ m.

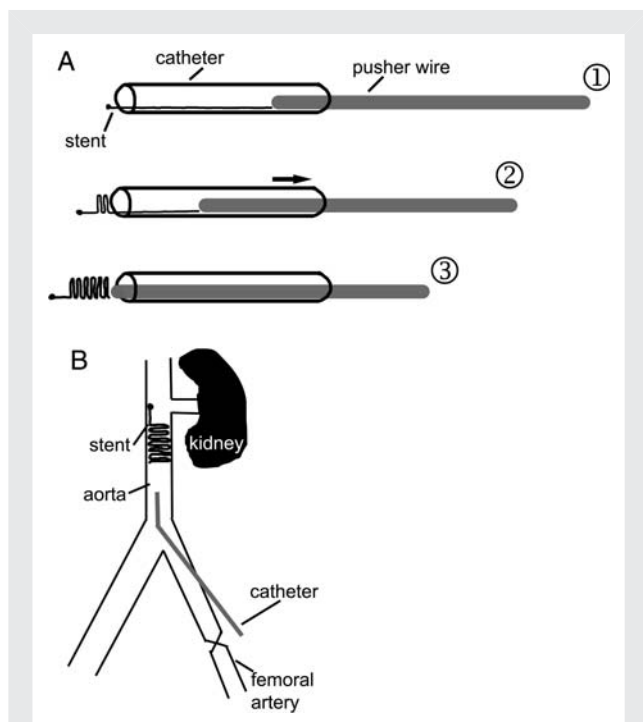


**Figure 2** Schematic diagram of stent deployment (A) and procedure (B). (A): (1) The straightened nitinol wire stent inside the catheter, with pusher wire, ready for insertion into the animal. (2) At point of deployment, catheter is retracted over the pusher wire to deploy the stent. The nitinol wire re-coils using shape memory. (3) Fully deployed stent. (B) The femoral artery is exposed and ligated distal from the aorta. Blood flow is temporarily stopped in the femoral using a sling and the stent catheter inserted through an arteriotomy. The catheter is pushed into the abdominal aorta before stent deployment. The catheter is then removed and the proximal femoral artery ligated.

48 h with aspirin (75 mg in 250 ml drinking water) and clopidogrel (25 mg/kg/day crushed and mixed with sardine). General anaesthesia was induced with isoflurane (maintenance rate of 1.5%) and analgesic (0.03 mg/ml vetergesic, s.c.) given. The mouse was positioned with its left hind limb fully extended and as in line with its spine as possible so as to create a straight line between femoral artery and aorta. An incision was made in the groin, and the femoral artery and vein exposed by blunt dissection. The vessels were bathed in a solution of 1% lidocaine hydrochloride, and the femoral nerve dissected free of the artery before the femoral vein and artery were controlled proximally with slings and ligated distally with 6/0 silk ties (Figure 1B). Following arteriotomy (Figure 1C), the stent catheter was inserted into the femoral artery (Figure 1D and E) and slowly advanced into the abdominal aorta. Insertion into the aorta was performed without visual guidance. However, measurement of dissected specimens of similar weights showed that the renal arteries were just over 20 mm from the groin. Thus, the stent catheter was inserted to a distance of 20 mm. The stent was deployed and the catheter withdrawn before ligation of the femoral artery proximal to the arteriotomy, the wound closed, and the animals allowed to recover. Double antiplatelet therapy was continued post-operatively until harvest.

As a control, sham-stent procedures ( $n = 6$ ) were also performed, following the stent protocol but without deployment of a stent.

## 2.4 Tissue processing and histological analysis

Animals ( $n = 8-12$  per timepoint) were killed and perfusion fixed 1 h, 1, 3, 7, and 28 days post-stenting. Stented sections were embedded in glycol methacrylate resin (Technovit 8100, TAAB laboratories) or modified Wolf methacrylate resin<sup>8</sup> (refer Supplementary material online) and transverse sections, 10  $\mu\text{m}$  thick, made using an Isomet 5000 diamond tipped saw and Metaserv 2000 grinder/polisher (Buehler). Morphometric analysis was performed on H&E and EVG stained sections, using Lucia digital analysis software.

Each aorta generated two to three sections of sufficient quality for analysis, all of which were used in neointimal area analysis.

## 2.5 Immunohistochemical analysis

Immunohistochemical analysis was performed to determine endothelial cells (vWF, Dako, UK), inflammatory cells (mac-387, Dako), and smooth muscle cells ( $\alpha$ -smooth muscle actin, Dako). Slides embedded in modified Wolf methylmethacrylate were deacrylated in xylene and 2-methoxyethylacetate, followed by rehydration in acetone and water, or rehydrated in ethanol, followed by a water wash for sections embedded in T8100 resin, prior to staining. Antigen retrieval, by heating to 80°C for 20 min in citrate buffer, pH6, was performed for vWF and mac-387 staining. Sections were incubated with primary antibody for 3 h at 37°C in PBS containing 10% normal serum. Positive staining was visualized using the ABC technique followed by New Fuschin. Sections were dry mounted using superglue, without counterstaining. Further details on antibody dilutions and incubation times for each stain are given in Supplementary material online, Table S1.

## 2.6 Statistics

Data are presented as mean  $\pm$  SEM. Timecourse data were analysed using a one-way ANOVA followed by a Bonferroni post test. A Student's *t*-test was used for comparison of IL-1R1<sup>-/-</sup> vs. IL-1R1<sup>+/+</sup> neointima formation.  $P < 0.05$  was considered significant.

## 3. Results

Several prototypes of stent were designed, developed, and tested. The final design was a coil with external diameter 1.0 mm, length 3.0 mm, and a low pitch; the latter reducing the number of rotations made by the stent during deployment. As the stent exits the catheter eccentrically and caused perforation of the vessel with initial prototypes, the tip was blunted with a laser welded bead, and a 1.0 mm straight 'leg' added to act as a stabilizing strut lying against the vessel wall during deployment, giving the stent a final length of 4.0 mm.

The stent was developed and tested in 42 animals. The final design was then deployed in 76 mice, with 69 resulting in successful recovery of a stented aorta. All arteries were patent upon harvest. The 9% of animals that failed were lost due to procedural problems. These involved failure of the stent to deploy from the catheter (four animals), failure to insert the catheter into the arteriotomy (two animals), and stent migration into the abdominal cavity (one animal).

The stent procedure can be undertaken with confidence after training on approximately six mice and takes 30 min to complete, in the hands of an experienced operator, with minimal blood loss. Excessive blood loss is controlled by slings providing a temporary

ligation to the vessels during the procedure. Once the catheter is inserted into the femoral artery, blood loss is prevented by the oversizing of the catheter compared with the vessel. A small amount of blood does flow through the catheter itself, but this is minimal (less than 5  $\mu\text{L}$ ).

The procedure has two areas where difficulty might occur. First, negotiating the bend between the femoral artery and aorta can be problematic. This is resolved by ensuring the mouse hind leg is as in line with the spine as possible during the procedure to create a straight line between the vessels. Also the outer diameter of the delivery catheter is critical: the tip of the stent protrudes from the catheter to aid insertion into the arteriotomy, and delivery catheters with a small outer diameter have proven more likely to hit resistance at the femoral/aorta branch, possibly due to the mechanics of the tube not holding the aorta wall off the stent itself during insertion.

The second procedural problem encountered is permanent leg paralysis in the mouse on recovery. This occurred in 22% of all mice undergoing the procedure, with a higher incidence (13%) during the initial development of the technique. Permanent paralysis is avoided by minimal manipulation of the femoral nerve during the procedure and ensuring the nerve is not caught up in any sutures of the vessels. Temporary paralysis of the hind leg upon immediate recovery is more common (29% of all mice) and is caused by the use of the local anaesthetic lidocaine hydrochloride during the procedure. The animals recover from this paralysis within 30–60 min post-procedure.

Evaluation of the timecourse of stenting showed a progressive development of neointima (Figures 3A and 4 and see Supplementary material online, Figure S1). At 1 day after stenting, polymorphonuclear cells are seen around the edge of the stent (Figure 4B). Inflammatory cells are also seen beneath the stent, in the adventitia. Thrombus formation, containing macrophages, is also evident (Figure 5A). A smooth neointimal accumulation was observed associated with the stent by 3 days. At 7 days, endothelial cells were seen lining the neointima (Figure 4D and 5B), which was still associated mainly with the stent. At 28 days post-stenting, however, a crescentic, organized, and mature neointima, consisting of smooth muscle cells, was seen (Figures 4 and 5). In contrast, sham-stented animals did not develop a neointima in their aorta after 28 days (Figure 4A). Neointimal area along the length of the each part of the aorta containing the coil stent was not significantly variable (minimum: 0.046, maximum: 0.064  $\text{mm}^2$ ; median: 0.059, SD: 0.008). Internal elastic lamina (IEL) area, mean strut area of each section, and medial thickness remained constant throughout the timecourse (data not shown). There was no change in body weight using this model.

To determine the usefulness of the mouse aortic stent model in interventional studies, we examined neointimal formation, 28 days post-stenting, in stented animals that were unable to signal via IL-1. IL-1R1<sup>-/-</sup> mice subjected to aortic stenting developed significantly less neointima than their wild-type control (Figure 3B). Medial thickness, total vessel area, and mean stent strut area did not differ between these two groups.

## 4. Discussion

This is the first description of a mouse model of *in situ* stenting, using a stent specifically tailored for use in small thin-walled

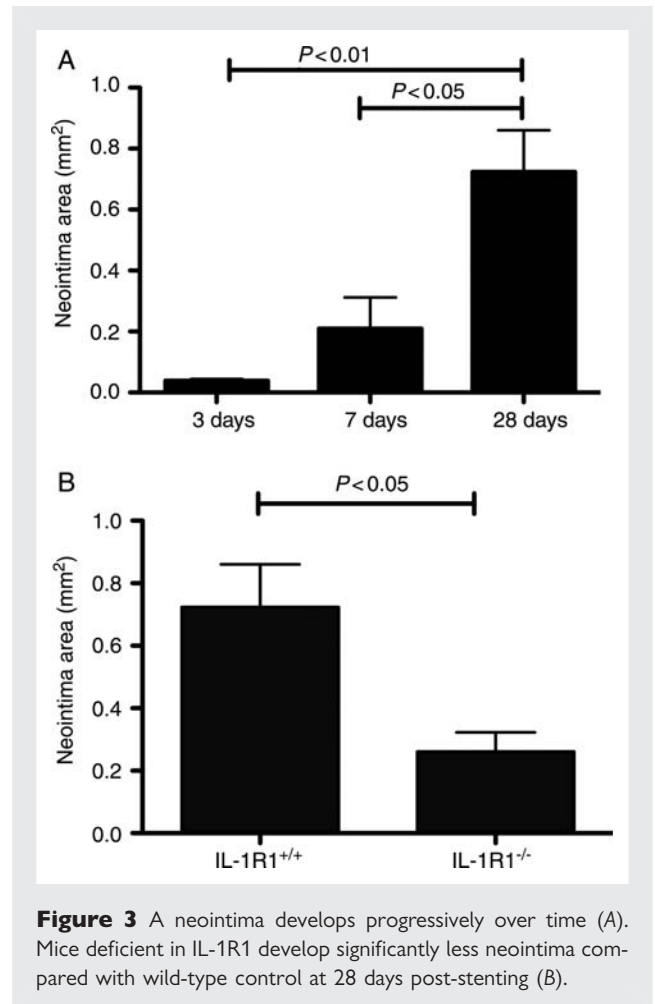


**Figure 3** A neointima develops progressively over time (A). Mice deficient in IL-1R1 develop significantly less neointima compared with wild-type control at 28 days post-stenting (B).

arteries. The model is a reliable and reproducible procedure that can be undertaken by a single operator without the need for an advanced level of microsurgical skill. All the vessels are patent at 28 days post-stenting, and a gradual accumulation of neointima is seen over the timecourse of 28 days, which is similar to the pattern seen in other rodent, rabbit, and pig models.<sup>5,9–21</sup> In addition, neointimal formation in stented animals that are deficient in IL-1 signalling is reduced compared with control animals, in agreement with studies using different models of arterial injury and other animal models of stenting.<sup>6,7</sup> Thus, the model described here is comparable with others currently in use and will be useful in interventional studies.

The stent used in our model is made from nitinol, a nickel titanium alloy that has shape memory. Thus, the stent is a self-expanding coil that reshapes, upon deployment, from the straight wire loaded into the introducer. Such a stent was in common use in human studies in the 1990s, although concerns were raised over toxicity to vascular smooth muscle cells on corrosion<sup>22</sup> and the capacity of the stent to continue to expand after deployment.<sup>23</sup> In our model, toxicity due to corrosion is not a concern, unless an extended timepoint is investigated, and the constant IEL area of sections throughout the timecourse of stenting, observed in our study, suggests that continued expansion is not occurring.



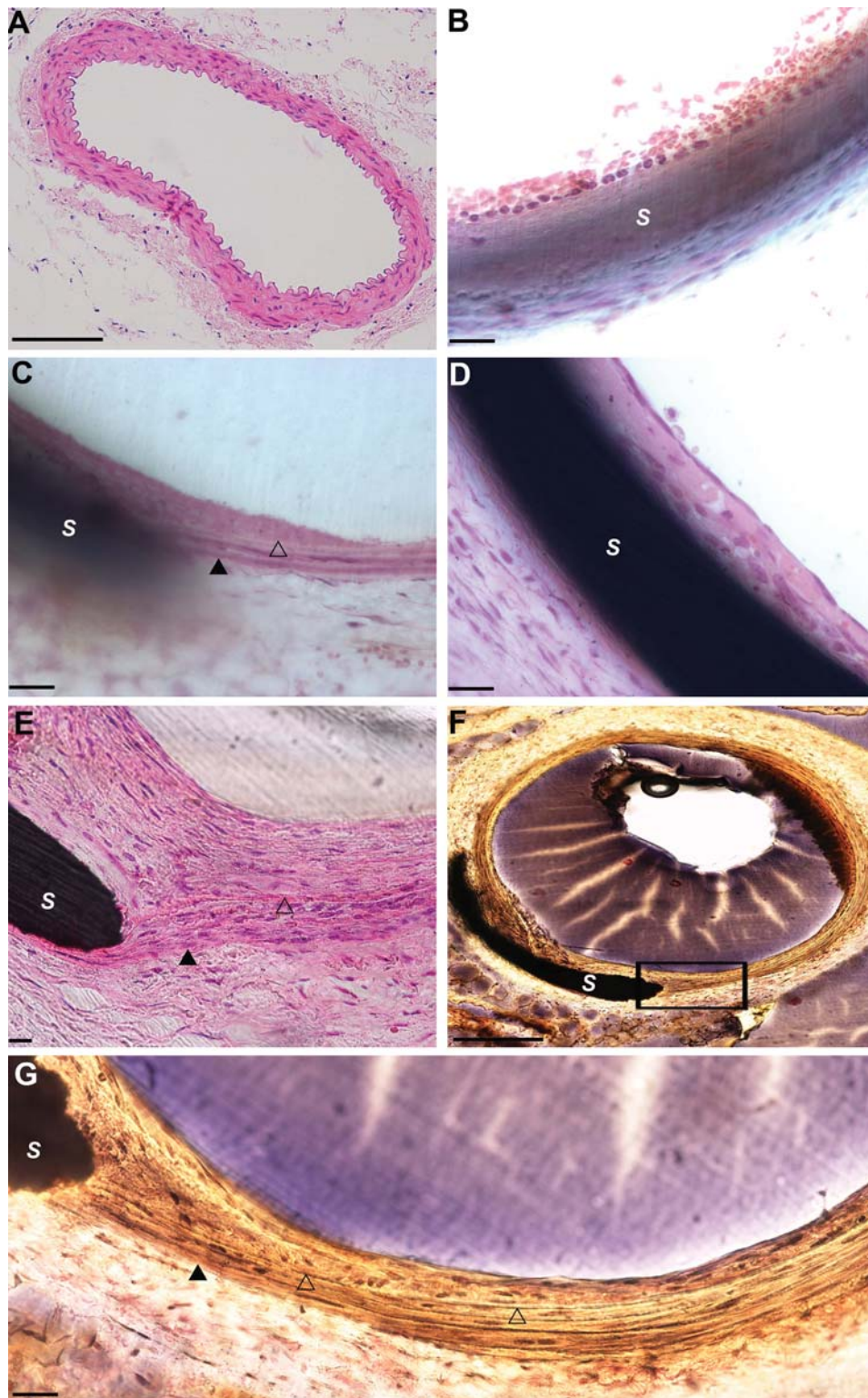


**Figure 4** Sham stented animals do not develop a neointima at 28 days (A). Polymorphonuclear cells are seen around the stent strut at 1 day post-stenting (B). A small neointima begins to form at 3 days (C). Endothelialization of the neointima is seen at 7 days (D). A mature neointima is seen at 28 days (E and F). Image G is a high power of the boxed area in F, stained with elastic van Gieson. Purple luminal stain is an artefact caused by the T8100 resin. Open triangles depict the IEL; filled triangles the external elastic lamina, S marks the stent. Scale bar represents 50  $\mu\text{m}$ .

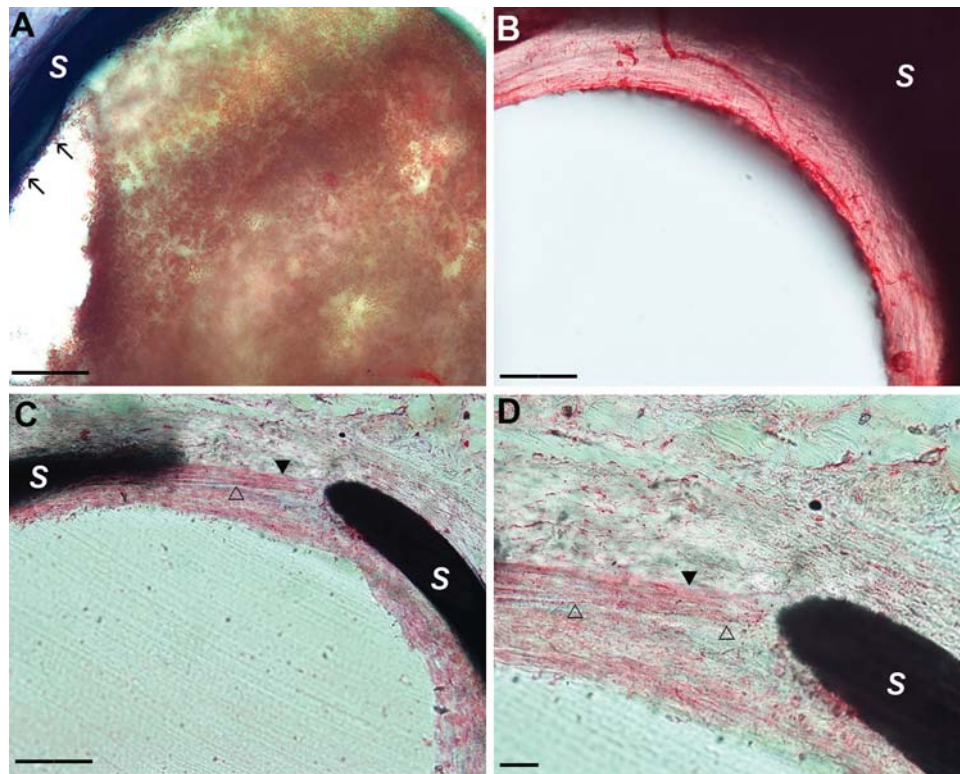


**Figure 5** Immunohistochemical staining showing inflammatory cells trapped in a transient thrombus and on the stented surface (arrowed) at 3 days (A), endothelial cells lining the lumen at 7 days (B), and smooth muscle cells of the media and neointima at 28 days post-stenting (C and D). Open triangles depict the IEL; filled triangles the external elastic lamina; and S denotes stent metal. Scale bar represents 100  $\mu\text{m}$ .

The presence of the coiled stent metal could potentially present a difficulty with analysis of sections using this model. However, the mean strut area of each section remains constant, as does the variability in neointima between sections. Thus, there is no significant variation between sections, despite the eccentric lesion in relation to the spiral shape of the stent, meaning that the model is both reproducible and reliable.

Mice are small, inexpensive, and easy to handle, making them ideal for use in disease models. Mice are also amenable to genetic manipulation and can be rendered susceptible to atherosclerosis.<sup>3,4</sup> Therefore, a mouse stent model will allow more detailed investigation into the development of in-stent restenosis following stenting of a diseased vessel. The mouse carotid is the best characterized vessel in models employing surrogate injuries, but is too small to stent. The aorta, like the carotid, is an elastic artery and is over twice the diameter of the carotid. The aorta, therefore, is currently the vessel of choice for a mouse stent model.

The aorta is also used in several rat models of stenting.<sup>11–14</sup> All these models use a commercially available balloon expandable stent rather than the coil stent used in our model. Two models involve substantial abdominal surgery, deploying the stent directly into the abdominal aorta via arteriotomy,<sup>11,13</sup> another deploys the stent into the thoracic aorta via carotid artery access,<sup>12</sup> and a fourth deploys the stent in the abdominal aorta via femoral

access in a procedure similar to the one described in our mouse model.<sup>14</sup> All these models report a failure rate of 8–15%, which is comparable to the 10% rate of our model. The neointima formation in all these models is modest and develops slowly over time, with the neointima mainly associated with the stent strut up to 7 days post-procedure. Inflammation is also apparent, associated with the stent struts, in these models up to 3 days after placement of the stent. This is directly comparable to our mouse model, which also has stent-associated inflammation and a small neointima that is initially associated with the stent before becoming a mature, concentric neointima at 28 days.

Only one other model of mouse stenting has been developed.<sup>5</sup> This model deploys a balloon expandable stent into the thoracic aorta of a donor mouse, which is subsequently grafted into the carotid circulation of a recipient mouse. This model demands a high level of microsurgical skill and uses two mice for each procedure. Our model, in contrast, employs a more simple technique in which a self-expanding stent is deployed ‘directly’ into the aorta of the mouse under investigation. Thus, the stent is deployed *in situ*, without complicating features of transplantation and marked changes in vessel diameter and flow dynamics. In addition, although our model involves an initial steep learning curve (equivalent to other reported models), it has a high rate of success (92% survival rate compared with 80–90% reported by other small animal models) and all vessels were patent on harvest.



Our model does have some limitations, which are common with other methods utilizing sections with the stent remaining *in situ*. The thickness of the stent sections obtained, along with the fact that the spiral coil stent rises out of the tissue in each section, leads to a difficulty in obtaining high-quality images. In addition, immunohistochemical staining is limited in tissue embedded in methylmethacrylate resin, which is further exacerbated by the thickness of the section obtained. This limits the ability to characterize events causing in-stent restenosis in this model and could limit its usefulness to investigations of efficacy of potential treatments. However, despite the limitations on immunostaining, we have managed to achieve positive staining for smooth muscle, inflammatory and endothelial cells, depending on the methylmethacrylate resin used, antigen retrieval, and an altered incubation protocol from the standard used with wax-embedded sections.

The usefulness of this model in interventional studies is shown by the response to stenting of mice deficient in IL-1 signalling, compared with wild-type mice. We have previously shown that these mice develop a significantly reduced neointima in response to carotid ligation injury,<sup>6</sup> a response that is duplicated using our stent model. Bone marrow transplant experiments in these mice suggest IL-1 signalling in both vascular wall cells and circulating (inflammatory and progenitor) cells play an equal role in neointima formation following carotid ligation,<sup>6</sup> and it is likely that the same mechanism is involved in in-stent restenosis, following stenting of these mice.

In conclusion, we have established a new model of *in situ* murine stenting. The model mimics features of neointimal formation in the human, and replicates those of other animal stent models. Thus, the model will allow investigation into molecular pathways in in-stent restenosis (using transgenic or chimeric mice), as well as novel anti-restenosis strategies.

## Supplementary material

Supplementary material is available at *Cardiovascular Research* online.

## Acknowledgements

The authors thank Keith Channon and Nick Alp, University of Oxford, for helpful discussion of the stent model.

**Conflict of interest:** H.L. is the Managing Director of Brivant Medical Engineering.

## Funding

This work was supported by the British Heart Foundation (PG/07/024). Funding to pay the Open Access publication charges for this article was provided by the British Heart Foundation.

## References

- Schwartz RS, Murphy JG, Edwards WD, Camrud AR, Vliestra RE, Holmes DR. Restenosis after balloon angioplasty. A practical proliferative model in porcine coronary arteries. *Circulation* 1990;**82**:2190–2200.
- Touchard AG, Schwartz RS. Preclinical restenosis models: challenges and successes. *Toxicol Pathol* 2006;**34**:11–18.
- Plump AS, Smith JD, Hayek T, Aalto-Setälä K, Walsh A, Verstuyft JG et al. Severe hypercholesterolemia and atherosclerosis in apolipoprotein E-deficient mice created by homologous recombination in ES cells. *Cell* 1992;**71**:343–353.
- Ishibashi S, Goldstein JL, Brown MS, Herz J, Burns DK. Massive xanthomatosis and atherosclerosis in cholesterol-fed low density lipoprotein receptor-negative mice. *J Clin Invest* 1994;**93**:1885–1893.
- Ali ZA, Alp NJ, Lupton H, Arnold N, Bannister T, Hu Y et al. Increased in-stent stenosis in ApoE knockout mice: insights from a novel mouse model of balloon angioplasty and stenting. *Arterioscler Thromb Vasc Biol* 2007;**27**:833–840.
- Chamberlain J, Evans D, King A, Dewberry R, Dower S, Crossman D et al. Interleukin-1beta and signaling of interleukin-1 in vascular wall and circulating cells modulates the extent of neointima formation in mice. *Am J Pathol* 2006;**168**:1396–1403.
- Morton AC, Arnold ND, Gunn J, Varcoe R, Francis SE, Dower SK et al. Interleukin-1 receptor antagonist alters the response to vessel wall injury in a porcine coronary artery model. *Cardiovasc Res* 2005;**68**:493–501.
- Wolf E, Roser K, Hahn M, Welkerling H, Delling G. Enzyme and immunohistochemistry on undecalcified bone and bone marrow biopsies after embedding in plastic: a new method for routine application. *Virchows Arch Pathol Anat* 1992;**420**:17–24.
- Finn AV, Gold HK, Tang A, Weber DK, Wight TN, Clermont A et al. A novel rat model of carotid artery stenting for the understanding of restenosis in metabolic diseases. *J Vasc Res* 2002;**39**:414–425.
- Indolfi C, Esposito G, Stabile E, Cavuto L, Pisani A, Coppola C et al. A new rat model of small vessel stenting. *Basic Res Cardiol* 2000;**95**:179–185.
- Langeveld B, Roks AJ, Tio RA, van Boven AJ, van der Want JJ, Henning RH et al. Rat abdominal aorta stenting: a new and reliable small animal model for in-stent restenosis. *J Vasc Res* 2004;**41**:377–386.
- Lowe HC, James B, Khachigian LM. A novel model of in-stent restenosis: rat aortic stenting. *Heart* 2005;**91**:393–395.
- Roks AJM, Henning RH, van Boven AJ, Tio RA, van Gilst WH. Rat abdominal aortic stenting: a simple model displaying in-stent restenosis. *Am J Cardiol* 2002;**89**:1149–1150.
- Jonas M, Edelman ER, Groothuis A, Baker AB, Seifert P, Rogers C. Vascular neointimal formation and signalling pathway activation in response to stent injury in insulin-resistant and diabetic animals. *Circ Res* 2005;**97**:725–733.
- Carter AJ, Farb A, Gould KE, Taylor AJ, Virmani R. The degree of neointimal formation after stent placement in atherosclerotic rabbit iliac arteries is dependent on the underlying plaque. *Cardiovasc Pathol* 1999;**8**:73–80.
- Feldman LJ, Mazighi M, Scheuble A, Deux JF, De Benedetti E, Badier-Commander C et al. Differential expression of matrix metalloproteinases after stent implantation and balloon angioplasty in the hypercholesterolemic rabbit. *Circulation* 2001;**103**:3117–3122.
- Kollum M, Kaiser S, Kinscherf R, Metz J, Kubler W, Hehrlein C. Apoptosis after stent implantation compared with balloon angioplasty in rabbits. Role of macrophages. *Arterioscler Thromb Vasc Biol* 1997;**17**:2383–2388.
- Kim WH, Hong MK, Virmani R, Kornowski R, Jones R, Leon MB. Histopathologic analysis of in-stent neointimal regression in a porcine coronary model. *Coron Artery Dis* 2000;**11**:273–277.
- Miller DD, Karim MA, Edwards WD, Schwartz RS. Relationship of vascular thrombosis and inflammatory leukocyte infiltration to neointimal growth following porcine coronary artery stent placement. *Atherosclerosis* 1996;**124**:145–155.
- Taylor AJ, Gorman PD, Kenwood B, Hudak C, Tashko G, Virmani R. A comparison of four stent designs on arterial injury, cellular proliferation, neointima formation, and arterial dimensions in an experimental porcine model. *Catheter Cardiovasc Interv* 2001;**53**:420–425.
- Schwartz RS, Huber KC, Murphy JG, Edwards WD, Camrud AR, Vliestra RE et al. Restenosis and the proportional neointimal response to coronary artery injury: results in a porcine model. *J Am Coll Cardiol* 1992;**19**:267–274.
- Shi C-C, Lin S-JL, Chen Y-L, Lai S-T, Wu GJ, Kwok C-F et al. The cytotoxicity of corrosion products of nitinol stent wire on cultured smooth muscle cells. *J Biomed Mater Res* 2000;**52**:395–403.
- Roguin A, Grenadier E, Linn S, Markiewicz W, Beyar R. Continued expansion of the nitinol self-expanding coronary stent: angiographic analysis and 1-year clinical follow-up. *Am Heart J* 1999;**138**:326–333.